Conjugated Polyions Enable Organic Photovoltaics Processed from Green Solvents

Ye, Gang; Doumon, Nutifafa Y.; Rousseva, Sylvia; Liu, Yuru; Abdu-Aguye, Mustapha; Loi, Maria A.; Hummelen, Jan C.; Koster, L. Jan Anton; Chiechi, Ryan C.

Published in:
ACS Applied Energy Materials

DOI:
10.1021/acsaem.8b02226

Publication date:
2019

ACS APPLIED ENERGY MATERIALS

Article

Cite This: ACS Appl. Energy Mater. 2019, 2, 2197−2204

www.acsaem.org

Conjugated Polyions Enable Organic Photovoltaics Processed from Green Solvents

Gang Ye,[†,‡] Nutifafa Y. Doumon,[‡] Sylvia Rousseva,[†,‡] Yuru Liu,[†,‡] Mustapha Abdu-Aguye,[‡] Maria A. Loi,[‡] Jan C. Hummelen,[†,‡] L. Jan Anton Koster,[‡] and Ryan C. Chiechi*[,†,‡]

[†]Stratingh Institute for Chemistry, University of Groningen, Nijenborgh 4, 9747 AG Groningen, The Netherlands

[‡]Zernike Institute for Advanced Materials, Nijenborgh 4, 9747 AG Groningen, The Netherlands

Supporting Information

ABSTRACT: This paper describes the design, synthesis, and optical and electronic properties of two conjugated polymers **CPIZ-B** and **CPIZ-T** that incorporate closed-shell cations into their conjugated backbones, balanced by anionic pendant groups. The zwitterionic nature of the polymers renders them soluble in and processable from polar, protic solvents to form semiconducting films that are not doped. These unique properties are confirmed by absorption and electron paramagnetic resonance spectroscopy. The energies of the unoccupied states respond to the tritylium moieties in the conjugated backbone, while the occupied states respond to the electron-donating ability of the uncharged, aromatic units in the backbone. Films cast from 80:20 HCOOH/H_2O by volume show good electron mobilities, enabling a photovoltaic effect in proof-of-concept, bilayer solar cells.

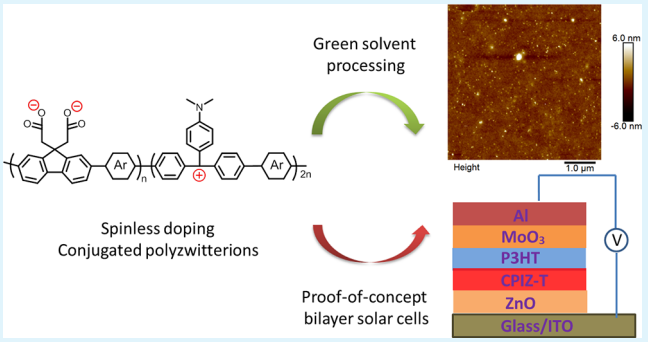

KEYWORDS: *conjugated polyions, opto-electronic devices, organic photovoltaics, intrinsic semiconductor, spinless doping*

1. INTRODUCTION

Conjugated polymers are solution-processable semiconductors, enabling the fabrication of thin-film devices such as field-effect transistors and organic solar cells (OSCs).[1−7] Although there is typically trade-off in performance compared to rigid, inorganic analogs, it is offset by the potential for inexpensive, large-scale device production, particularly from nontoxic, renewable, or otherwise green solvents.[8−11] However, these solvents tend to be polar and protic, e.g., water/ethanol mixtures, and conjugated polymers typically contain rigid, nonpolar aromatic rings. Although installing polar, ionic pendant groups can increase processability in these solvents,[12−14] the combination of nonpolar backbones with polar/ionic pendant groups[15−17] to form so-called conjugated polyelectrolytes (CPEs) drives aggregation and self-assembly in solution (akin to the folding of polypeptides in water) that negatively impacts their semiconducting properties; the polymer chains are not directly solubilized as, for example, a polysaccharide is in water. Thus, CPEs are generally more useful as ultrathin[18−23] interlayer materials to facilitate hole/electron extraction at the electrodes[10,18,19,21,24−26] rather than in the active layer of OSCs.[27,28] Thicker films tend to translate solution-phase aggregation into poor morphology, leading to low charge-carrier mobility.[29] Using doped CPEs mitigates some of these problems[30−35] but puts the polymers in the metallic state, precluding their use in OSCs.[36]

We are developing an alternative to CPEs in which "spinless doping" introduces formal charges into the backbones of conjugated polymers without the requisite spin to induce the transition to the metallic state.[37] These conjugated polyions (CPIs) are intrinsic semiconductors that are completely soluble in and processable from polar, protic solvents.[38−40] However, their redox potentials and bandgaps are not suitable for use in OSCs. In this work, we report two CPIs, **CPIZ-B** and **CPIZ-T**, synthesized using the three-component, random Suzuki−Miyaura copolymerization shown in Figure 1 to control the electronic structure while retaining sufficient ionic character in the backbone for processing from polar, protic solvents. Both **CPIZ-B** and **CPIZ-T** contain triarylmethane dyes in the leuco and the salt forms as components in the backbone, as has been reported previously.[41] The inclusion of these types of chromophores in the backbones of polymers leads to broad absorption in the visible spectrum and large extinction coefficients, which is beneficial for solar cells applications.[42] We verified the spinless doping process of our CPIs using ultraviolet−visible−near-infrared (UV−vis−NIR) and electron paramagnetic resonance (EPR) spectroscopy. We prepared the OSCs by casting films of **CPIZ-T** from mixtures of water and formic acid (HCOOH), acidic solutions being

Received: December 21, 2018
Accepted: February 8, 2019
Published: February 8, 2019

DOI: 10.1021/acsaem.8b02226
ACS Appl. Energy Mater. 2019, 2, 2197−2204

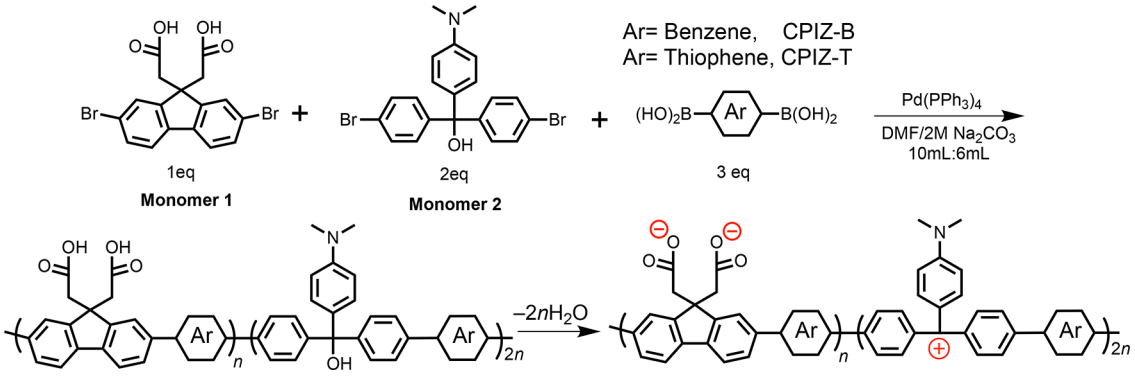

Figure 1. Synthesis of conjugated polyions via three-component random Suzuki−Miyaura copolymerization. The zwitterionic form is favored in the solid state by the loss of H_2O.

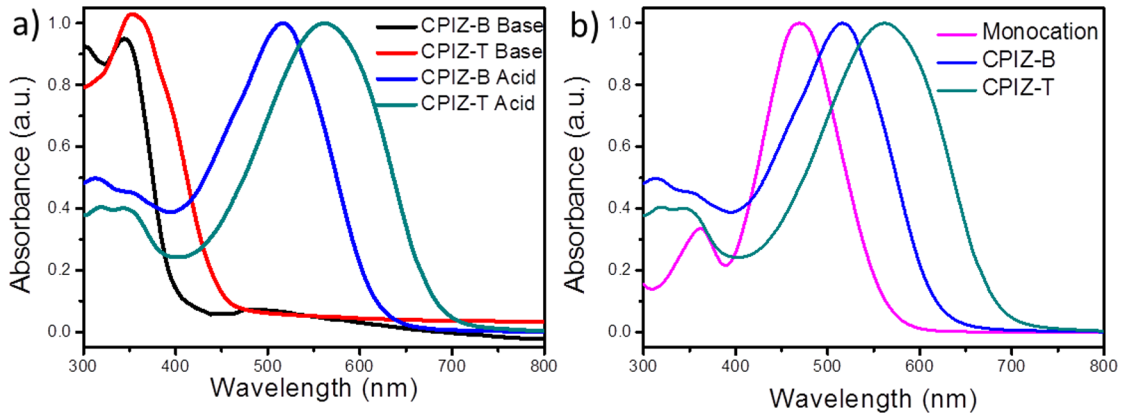

Figure 2. (a) Absorption spectra of the as-prepared conjugated polyions dissolved in either basic or acidic solutions, showing a pronounced bathrochromic shift in pure HCOOH (an acidic solution) corresponding to the formation of delocalized cations. (b) Absorption spectra of the monocation of monomer 2 and the **CPIZ-B** and **CPIZ-T** polymers in pure HCOOH.

necessary to prevent the cations from being quenched by water. Formic acid is naturally occurring and is widely used for industrial and agricultural applications and as a food additive. Although pure formic acid is corrosive and flammable, it is miscible with water and is nonflammable below 85% weight-percent (wt %), making 80:20 v% HCOOH/H_2O solutions a viable green solvent for processing organic semiconductors. We prove the utility of CPIs cast from these solvents by preparing bilayer OSCs.

2. RESULTS AND DISCUSSION

2.1. Synthesis and Characterization. In our previous work, we synthesized CPIs from aromatic polyketones by Friedel−Crafts (F−C) polymerization followed by nucleophilic addition to convert the resulting polyketone to a polyalcohol. Subsequent treatment with a Lewis acid or dehydrating agent effected spinless doping; however, F−C conditions limited the choice of polar/ionic pendant groups.[38,40] In this work, we used a three-component palladium-catalyzed Suzuki−Miyaura polymerization in wet DMF to avoid the limitations of F−C conditions and the intermediate polyketone entirely. Using this approach, we can also control the relative amounts of cationic and electron donating/withdrawing groups by separating them into different monomers. Monomer 1 provides the ionic pendant groups. Monomer 2 is a carbocation precursor, and monomer 3 is a diboronic acid decorated with aromatic units used to tune the bandgap as shown in Figure 1.

As synthesized, both polymers are insoluble in nonpolar solvents and only sparingly soluble in polar solvents; however, impurities and low-molecular-weight fractions can be removed by dialysis in water, after which **CPIZ-B** spontaneously undergoes spinless doping via loss of H_2O (Figure 1). As spinless doping reduces the bandgap, this process is commensurate with a color change from very light yellow to red, while **CPIZ-T** remains yellow even after dialysis. Both polymers are stable in pure HCOOH and stronger acids in which they both become deeply colored. The solubility of **CPIZ-B** is 10 mg mL^{-1} in pure HCOOH and 5 mg mL^{-1} in 80:20 v% HCOOH/H_2O. The solubility of **CPIZ-T** is somewhat higher, 20 mg mL^{-1} and 14 mg mL^{-1}, respectively. Although these solubilities are sufficient for processing into thin films, their low solubility in common organic solvents precluded the accurate determination of molecular weight by gel permeation chromatography (GPC). We verified the structures by NMR in CF_3COOD and followed the spinless doping process spectroscopically, which is explained in detail in the Supporting Information.

2.2. Photophysical Properties. The formation of cations in the backbone of a CPI (spinless doping) converts sp^3 carbons to sp^2, increasing the degree of conjugation and decreasing the bandgap,[38] which is clearly evident in the UV−vis absorption spectra of **CPIZ-B** and **CPIZ-T** in acidic and basic solutions shown in Figure 2a. Basic solutions of the two polymers are colorless and pale yellow, respectively; both are deeply colored in pure HCOOH. Note that polymers are not

DOI: 10.1021/acsaem.8b02226
ACS Appl. Energy Mater. 2019, 2, 2197−2204

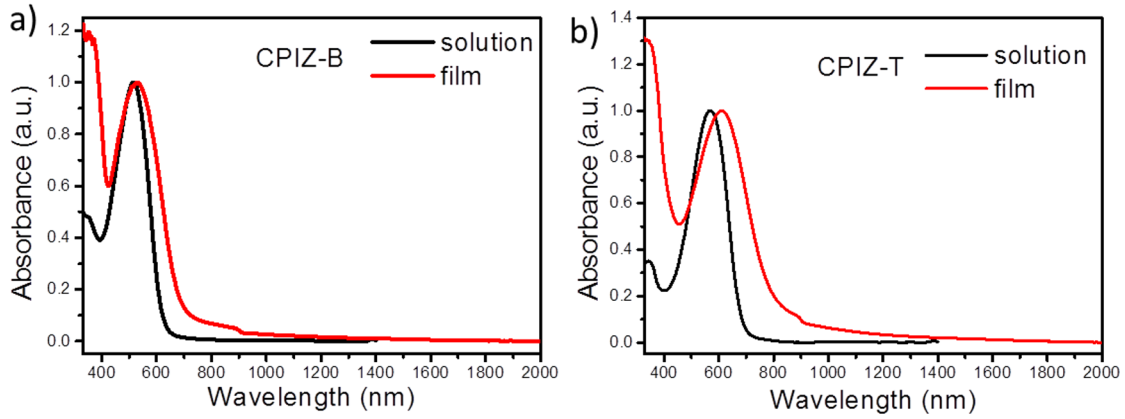

Figure 3. Absorption spectra of conjugated polyzwitterions **CPIZ-B** (a) and **CPIZ-T** (b) in HCOOH solution and thin film state as cast from HCOOH. No polaron and bipolaron absorption were observed in NIR region. The higher red shift of **CPIZ-T** compared with that of **CPIZ-B** indicates that **CPIZ-T** has better packing state.

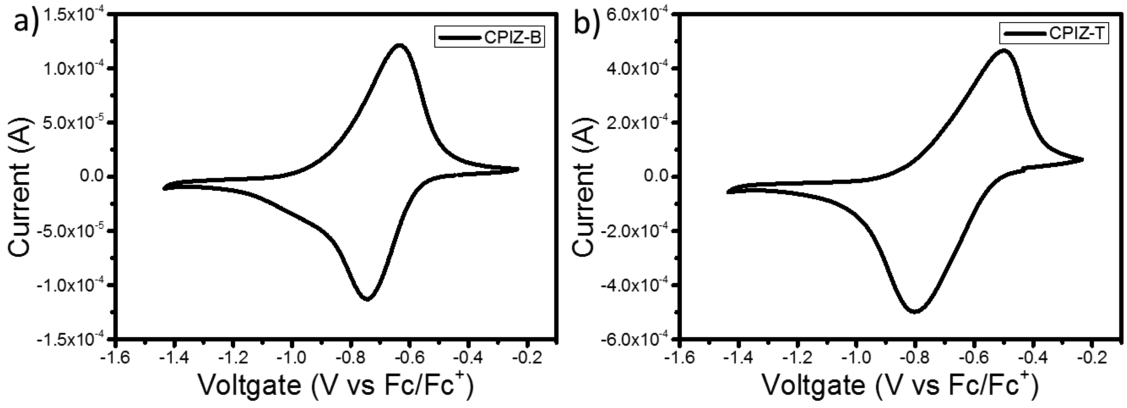

Figure 4. Cyclic voltammograms of a thin film of **CPIZ-B** (a) and **CPIZ-T** (b) versus Fc/Fc^+ on a glassy carbon working electrode immersed in 0.1 mol L^{-1} *n*-Bu_4NPF_6 acetonitrile solution at 100 mV s^{-1}. The fully reversible reduction waves are indicative of traditional redox doping/dedoping of the band structure of a semiconducting state conjugated polymer. In this case, **CPIZ-B** and **CPIZ-T** are being n-doped (reduced) and produce the p-doped (radical cationic) state due to semiconducting state of **CPIZ-B** and **CPIZ-T** having closed-shell cationic charges.

interconverting between the colorless and colored forms, rather, when as-prepared **CPIZ-B** and **CPIZ-T** are dissolved in basic solutions, they remain colorless. When they are dissolved in acidic solutions, they become deeply colored. The absorption maximum of the monocation formed from monomer 2 is significantly blue-shifted compared to the polymers (Figure 2b), demonstrating the effect of conjugation; the cations delocalize into the band structure. The $\pi-\pi^*$ transition at 300−400 nm is present in monomer 2 and the polymers, but the band at 468 nm in the monomer is replaced by an intraband transition at 500−700 nm that can be ascribed to charge-transfer between the electron-rich aromatic units and the electron-withdrawing tritylium unit (i.e., they function as donor/acceptor units). The shift in λ_{max} from 515 nm for **CPIZ-B** to 568 nm for **CPIZ-T** reflects the stronger donor character of thiophene compared to benzene.

Figure 3 shows the UV−vis−NIR spectra of **CPIZ-B** and **CPIZ-T** in pure HCOOH and in thin films. The spectra are featureless above ∼800 nm, indicating the absence of polarons or bipolarons, which is further confirmed by EPR and the lack of fluorescence quenching (see Supporting Information). In thin films, λ_{max} shifts to lower energies for both polymers, which is typical for conjugated polymers. The larger shift for **CPIZ-T** (44 nm compared to 17 nm) is likely due to the increased planarity afforded by the thiophene rings. The onsets in absorption correspond to bandgaps (E_g) of 1.82 and 1.57 eV for **CPIZ-B** and **CPIZ-T**, respectively.

2.3. Electrochemical Properties. For further insight into the electrochemical properties of **CPIZ-B** and **CPIZ-T**, we performed cyclic voltammetry (CV) under an inert atmosphere with a glassy carbon working electrode, a platinum wire counter electrode, and an Ag/AgCl pseudoreference electrode calibrated with ferrocene in 0.1 mol L^{-1} tetra-*n*-butylammonium hexafluorophosphate (*n*-Bu_4NPF_6) in CH_3CN as the supporting electrolyte. Spectra of films of **CPIZ-B** and **CPIZ-T** drop-cast from pure HCOOH onto the working electrode are shown in Figure 4. Both polymers exhibit fully reversible reduction waves corresponding to n-doping (reduction), which counterintuitively produces formally p-doped polymers due to their cationic nature in the pristine state. The half-wave reduction potentials ($E^{red}_{1/2}$) and the estimated valence and conduction band energies of **CPIZ-B** and **CPIZ-T** are listed in Table 1. We assigned an absolute energy of −4.8 eV to the ferrocene oxidation wave to reference $E^{red}_{1/2}$ to vacuum. The respective half-wave reduction peaks of **CPIZ-B** and **CPIZ-T** of −0.69 V and −0.65 V correspond to conduction band energies of −4.11 eV and −4.15 eV. These low-lying bands are the result of the positive charges introduced into the band structure by the tritylium residues. We calculated the valence bands by subtracting E_g from the absorption spectra from the

DOI: 10.1021/acsaem.8b02226
ACS Appl. Energy Mater. 2019, 2, 2197−2204

Table 1. Summary of Photophysical Properties, Electrochemical Properties, and Electron Mobilities of CPIZ-B and CPIZ-T

physical property	CPIZ-B	CPIZ-T
λ_{max} solution (nm)	515	568
λ_{max} film (nm)	532	612
λ_{onset} film (nm)	681	790
E_g optical[a] (eV)	1.82	1.57
$E_{1/2}^{red}$ (V)	−0.69	−0.65
conduction band from CV (eV)	−4.11	−4.15
valence band from CV/UV−vis (eV)	−5.93	−5.72
electron mobility[b] ($cm^2\ V^{-1}\ s$)	3.7×10^{-7}	2.0×10^{-4}
electron mobility[c] ($cm^2\ V^{-1}\ s$)	2.3×10^{-7}	2.5×10^{-4}

[a]Calculated from thin film absorption onset: $E_g = 1240/\lambda_{onset}$. [b]Cast from pure HCOOH. [c]Cast from 80:20 v% $HCOOH/H_2O$.

valence band energies, giving −5.93 eV and −5.72 eV for **CPIZ-B** and **CPIZ-T**, respectively. The larger difference in the valence band energies compared to the conduction bands is due to the electron-donating ability of thiophene. The absolute energies of the conduction bands of both polymers are close to the LUMO of the well-known fullerene acceptor PCBM, indicating that **CPIZ-B** and **CPIZ-T** are acceptor materials.

2.4. Density Functional Theory Calculation. To gain insight into the donor/acceptor character of **CPIZ-B** and **CPIZ-T**, we carried out density functional theory (DFT) calculations at the B3LYP/6-31G(d,p) level using Gaussian 09.[43] To simplify the calculations and because we determined the band energies experimentally, we considered only one repeat-unit comprising two cations. As can be seen in Figure 5, the HOMOs (which form the valence bands) are localized on the neutral fluorene moieties, while the LUMOs (which form the conduction bands) are localized on the cationic tritylium moieties. The structures without isoplots are shown in Figure S13. While neither structure is completely planar, the energy-minimized dihedral angles between the plane of the benzene bridge unit with neighboring plane of arene units are 39° for the fluorene block and 32° for tritylium block in **CPIZ-B**. In **CPIZ-T**, the dihedral angles between thiophene bridge unit with neighboring plane of arene units are 24° for the fluorene block and 8° for tritylium block. The smaller dihedral angles for the latter support the hypothesis that the smaller E_g of **CPIZ-T** in solution and in thin films is due to both the electron-donating ability of thiophene pushing the conduction band up and the increased planarity. The latter should lead to better packing in the solid state and explains the higher electron mobility of **CPIZ-T** (Table 1).

2.5. Device Performance. *2.5.1. Film Morphology.* One of the major impediments to fabricating OSCs with CPEs as the active layer is that the mismatch between the nonpolar main-chain and the ionic pendant groups in CPEs tends to result in poor morphologies when cast from solution. The inverse situation (CPIs with nonpolar pendant groups) creates the same problem.[40] The zwitterionic nature of **CPIZ-B** and **CPIZ-T** eliminates this problem by matching ionic backbones to ionic pendant groups. Figure 6 shows atomic force microscopy (AFM) images of **CPIZ-B** and **CPIZ-T** on bare glass substrates. Both polymers form smooth films when spin-coated from 5 mg mL^{-1} in HCOOH for **CPIZ-B** (rms roughness 1.82 nm) and 10 mg mL^{-1} in HCOOH for **CPIZ-T** (rms roughness 0.69 nm). When spun from more concentrated solutions, films of **CPIZ-B** became rough (rms roughness 4.68 nm, Figure S11).

2.5.2. Electron Mobility. We used the space-charge-limited-current (SCLC) method to extract the electron mobilities of single carrier electron-only devices made from the thin films of **CPIZ-B** and **CPIZ-T** cast from pure HCOOH and HCOOH with 20 v% of water. Electron mobilities were derived by fitting the measured room temperature current density−voltage characteristics of the fabricated electron-only devices to the modified Mott−Gurney equation:

$$J = \frac{9}{8}\varepsilon_0\varepsilon_r\mu_{0n}\exp\left(0.89\,\gamma(T)\sqrt{\frac{V}{L}}\right)\frac{V^2}{L^3} \quad (1)$$

where J is the electron current density, ε_0 and ε_r are the permittivity of free space and relative dielectric constant of the active layer respectively, μ_{0n} is the zero-field charge carrier mobility, L is the thickness of the device, $\gamma(T)$ is the temperature dependent electric field-activation factor, and V is the (applied) internal voltage corrected for V_{bi}, the built-in voltage, and V_{rs}, the voltage drop due to the series resistance of the contacts.

The J/V curves of **CPIZ-B** and **CPIZ-T**, corrected for the built-in voltage of V_{bi}, are shown in Figure 7. All of the J/V curves of **CPIZ-B** and **CPIZ-T** show a quadratic dependence of J on V, which is a characteristic of SCLC measurements. The mobility values are summarized in the Table 1. Both polymers exhibited similar electron mobilities in films cast

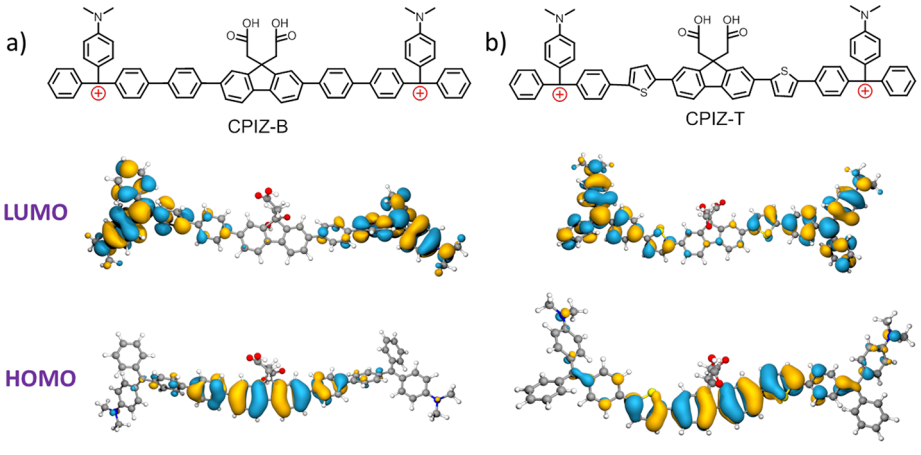

Figure 5. DFT-optimized molecular orbitals of **CPIZ-B** and **CPIZ-T**.

DOI: 10.1021/acsaem.8b02226
ACS Appl. Energy Mater. 2019, 2, 2197−2204

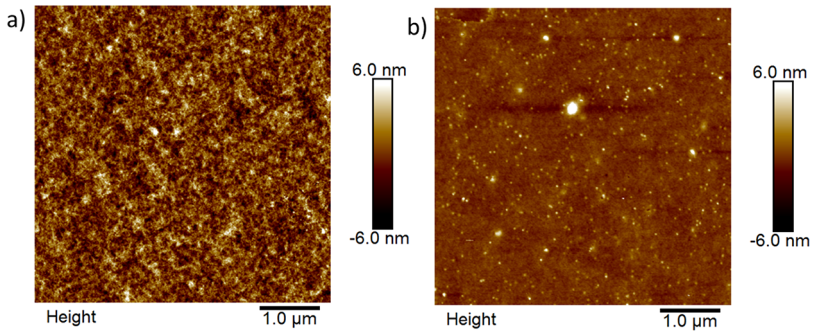

Figure 6. Surface topographic AFM image of (a) **CPIZ-B** and (b) **CPIZ-T** on bare glass surface (25 μm^2). The rms values are 1.82 and 0.69 nm for **CPIZ-B** and **CPIZ-T**.

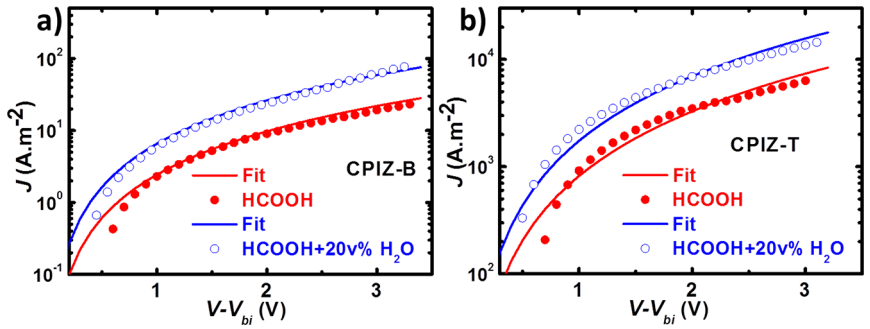

Figure 7. Current−voltage characteristics of electron-only devices for thin films of (a) **CPIZ-B** cast from pure HCOOH (70 nm thick; red circles) and from 80:20 v% HCOOH/H_2O (50 nm thick; blue circles) and (b) **CPIZ-T** cast from pure HCOOH (90 nm thick; red circles) and from 80:20 v% HCOOH/H_2O (70 nm thick; blue circles). Experimental data (circles) are fitted with SCLC current using eq 1 (solid lines).

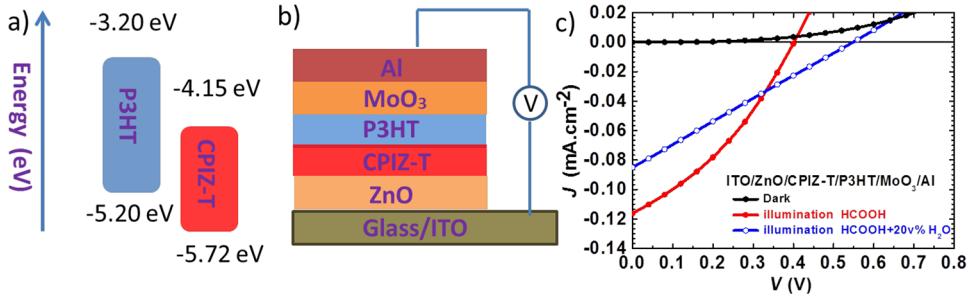

Figure 8. (a) Energy levels of P3HT and **CPIZ-T**, (b) illustration of the device structure, and (c) J/V curves.

from pure HCOOH and from 80:20 v% HCOOH/H_2O which, as discussed above, is nontoxic and nonflammable. However, the mobility of **CPIZ-T** is 3 orders of magnitude higher than **CPIZ-B**, which we ascribe to the influence of the thiophene.

As is depicted in Figure 1, treatment of the as-prepared CPIs with acid leads to the stoichiometric loss of H_2O, resulting in a zwitterionic polymer; however, in solution there will be an equillibrium concentration of $HCOO^-$ and protonated pendant RCOOH groups. Both H_2O and HCOOH are sufficiently volatile that they should be driven from the film in the solid-state, leaving the polymer in the purely zwitterionic form. To verify that significant amounts of mobile ions do not indeed remain in the films, we verified the lack of hysteresis in the trace-retrace J/V plots (Figure S14) and measured the impedance of **CPIZ-T** (Figure S15). Impedance spectroscopy provides a comprehensive insight into the basic mechanism of charge-transport. Any significant contributions from ion-conduction to the total conductivity of the film would manifest as a change in the phase shift in the low frequency range of the Bode plot and additional semicircles in the Nyquist impedance plot and/or give rise to a capacitive tail at low frequencies.[27,44] We observed no evidence of ionic conductivity in the Bode plot and Nyquist plot in the complex impedance plane of ITO/**CPIZ-T**/Al devices (Figure S16). The latter results in only one semicircle, which can be attributed to an equivalent circuit with a resistor parallel to a capacitor and is typical of ordinary semiconducting materials.

2.5.3. Bilayer Solar Cells. The properties of **CPIZ-B** and **CPIZ-T** elucidated thus far suggest that they should function as acceptors in OSCs with poly(3-hexylthiophene) [P3HT] as a donor (Figure 8a). Ideally, we would test the performance of **CPIZ-T** in bulk-heterojunction OSCs, but that would require a donor material that could be cast from HCOOH. Thus, we fabricated inverted bilayer ITO/ZnO/**CPIZ-T**/P3HT/MoO_3/Al OSCs in the configuration shown in Figure 8b, in which ZnO and MoO_3 act as electron and hole transporting layers, respectively. Figure 8c shows the J/V curves for the devices under dark and AM 1.5G illumination at 100 mW/cm^2, and Table 2 summarizes the device characteristics. Control devices

DOI: 10.1021/acsaem.8b02226
ACS Appl. Energy Mater. 2019, 2, 2197−2204

Table 2. Photovoltaic Parameters of the Bilayers Devices Based on CPIZ-T and P3HT

active layer	solvent	J_{sc} [mA/cm^2]	V_{oc} [V]	FF [%]	PCE [%]
P3HT	C_6H_5Cl	0.663	0.197	26	0.03
CPIZ-T	HCOOH	0.111	0	0	0
CPIZ-T/P3HT	HCOOH	0.116	0.402	34.4	0.02
CPIZ-T/P3HT	80:20 v% HCOOH/H_2O	0.085	0.548	24.7	0.01

with only a layer of **CPIZ-T** produced no measurable open-circuit voltage (V_{oc}), fill-factor (FF), or power conversion efficiency (PCE). Bilayer solar cells devices in which **CPIZ-T** was cast from HCOOH or 80:20 v% HCOOH/H_2O yielded PCEs of 0.02% and 0.01%, respectively.

The low V_{oc} is likely due to the nonideal match between the conduction bands of P3HT and **CPIZ-T**. The low FF is a consequence of the bilayer architecture. As a proof-of-concept, however, the results unambiguously demonstrate that CPIs cast from green solvents are viable active-layer materials for OSCs. To contextualize these results, the first bilayer OSCs that used conjugated polymers as donors gave PCEs of 0.04%,[45] which increased to 2.9% by blending the materials in a bulk-heterojunction.[46]

To demonstrate that **CPIZ-T** actively contributes to a photovoltaic effect at the interface between the donor and acceptor films, we additionally prepared ITO/ZnO/P3HT/MoO_3/Al devices. These P3HT-only devices give a comparable PCE of the bilayer (0.03%), which is primarily the result of the higher mobility of ZnO compared to **CPIZ-T** leading to a higher J_{sc}. The V_{oc} of the P3HT-only device is only 0.197 V compared to 0.548 V for the P3HT/**CPIZ-T** bilayer device. This significant difference in V_{oc} is unambiguous evidence that the PCE in the bilayer devices is driven by a photovoltaic effect at the P3HT/**CPIZ-T** interface.

3. CONCLUSION

Processing OSCs from nonrenewable organic solvents does not preclude their technological or commercial viability. However, processing from nontoxic, nonflammable renewable solvents will, in principle, bring down the costs and carbon payback of future OSC technology. We present CPIs as a viable pathway toward that end via proof-of-concept bilayer OSCs in which the CPI acceptor layer is cast from 80:20 v% HCOOH/H_2O. The zwitterionic nature of the CPIs, in which opposing charges exist in the backbone and pendant groups, imparts not just processability but also solubility in polar, protic solvents. Although they bear charges in the band structure, CPIs are intrinsic semiconductors, as evidenced by the dependence of the bandgap on the degree of charge in the backbone and the lack of unpaired spins determined by ESR spectroscopy. Although the absolute efficiencies of the bilayer OSC devices are low by modern standards, they are similar to those of bilayer OSCs that use conventional conjugated polymers processed from standard organic solvents. We are working to develop CPIs that function as donors, which would allow the processing of bulk heterojunction blends from green solvents that will, in principle, produce technologically relevant efficiencies from active layers processed entirely from green solvents.

4. EXPERIMENTAL SECTION

4.1. Device Fabrication. Although HCOOH is nontoxic, it is both volatile and caustic, and skin or eye contact to either the liquid or vapor should be avoided. In concentrations above 85% it is also flammable. Working with the concentrated HCOOH solutions described in this paper requires gloves, proper clothing, and eye protection and should only be done in a chemical fume hood.

4.1.1. Electron-Only Devices. The electron only devices were made similar to our previous work.[47] Glass substrates were cleaned in warm soap solution and rinsed successively in water, acetone, and isopropanol and then spin-dried and baked at 140 °C for about 10 min. The clean glass substrates were transferred into the evaporator kept at high vacuum (around 10^{-7} mbar) where a 20 nm thick aluminum (Al) film was deposited atop the glass substrates after which they were exposed to air for about 10 min. The prepatterned Al glass was then transferred into a nitrogen filled glovebox. The active layer films were spin coated from 10 mg mL^{-1} solutions of CPIZs in HCOOH and HCOOH with 20 v% of water, yielding 70 and 90 nm, respectively, for **CPIZ-B** and **CPIZ-T** in HCOOH with about 20 nm reduction in thickness for the films spin coated from solutions with 20 v% of water. Finally, the devices were completed by thermal evaporation of a 1 nm thick LiF and a 100 nm thick Al top electrodes under vacuum (around 10^{-7} mbar) in a glovebox. The final device structure is Al/**CPIZ-B** or **CPIZ-T**/LiF/Al. The J/V characteristics of the devices were measured in dark mode at room temperature in nitrogen filled glovebox with O_2 and H_2O levels kept below 0.1 ppm. A Keithley 2400 source meter was used to acquire the current−voltage data by applying a bias in the range of −3 to 3 V while recording the corresponding currents.

4.1.2. Bilayer Solar Cells. The cleaning steps for the solar cells are as described above except that the substrates are prepatterned ITO glasses. A 30 nm layer of ZnO was spin coated from sol gel solution and annealed at 170 °C for 30 min. The zinc oxide solution was prepared by dissolving 109.67 mg of zinc acetate in 1 mL of 2-methoxyethanol and 0.0302 mL of ethanolamine. Then the solution was stirred at room temperature for few hours. Then a layer of **CPIZ-T** was spin coated atop the ZnO layer from 10 mg mL^{-1} solution of **CPIZ-T** in HCOOH and HCOOH with 20 v% of water. The **CPIZ-T** layer processed from HCOOH with 20 v% of water was annealed at 100 °C for 10 min. Atop the **CPIZ-T** layer, a second layer from 20 mg mL^{-1} solution of P3HT in chlorobenzene was spin coated. To complete the device, the samples were transferred into an evaporator kept under vacuum (around 10^{-7} mbar) overnight and finished with thermal evaporation of a 10 nm thick MoOx and a 100 nm thick Al. The final structure is ITO/ZnO/**CPIZ-T**/P3HT/MoOx/Al. The cells were annealed at 150 °C for 30 min. The J/V characteristics were similarly taken as described above under 1 sun illumination.

4.2. Impedance Spectroscopy Measurements. Commercially available glass substrates patterned with ITO were cleaned in warm soap solution and rinsed successively in water, acetone, and isopropanol and then spin-dried, baked at 140°C for about 10 min, and treated in UV−ozone for 20 min. **CPIZ-T** solutions were made: 10 mg mL^{-1} of **CPIZ-T** in HCOOH and filtered with a 5 μm filter. The active layer was spin coated directly atop the cleaned ITO substrates from the filtered **CPIZ-T** solutions. The Al top electrodes were deposited with thermal evaporation of Al (100 nm) in a glovebox under vacuum (around 10^{-7} mbar). The structure of the devices is ITO/**CPIZ-T**(80 nm)/Al(100 nm). Impedance spectroscopy was carried out using a Solatron 1260 impedance gain-phase analyzer with an AC drive voltage of 10 mV in the range of 1 Hz to 1 MHz.

DOI: 10.1021/acsaem.8b02226
ACS Appl. Energy Mater. 2019, 2, 2197−2204

■ ASSOCIATED CONTENT

Supporting Information

The Supporting Information is available free of charge on the ACS Publications website at DOI: 10.1021/acsaem.8b02226.

Detailed description of the synthesis and characterization; details of density functional theory calculations; impedance and conductance measurements (PDF)

■ AUTHOR INFORMATION

Corresponding Author

*E-mail: r.c.chiechi@rug.nl.

ORCID

Nutifafa Y. Doumon: 0000-0002-2625-1647
Maria A. Loi: 0000-0002-7985-7431
L. Jan Anton Koster: 0000-0002-6558-5295
Ryan C. Chiechi: 0000-0002-0895-2095

Notes

The authors declare no competing financial interest.

■ ACKNOWLEDGMENTS

This work is part of the research program of the Foundation for Fundamental Research on Matter (FOM), which is part of The Netherlands Organization for Scientific Research (NWO). This is a publication by the FOM Focus Group "Next Generation Organic Photovoltaics", participating in the Dutch Institute for Fundamental Energy. G.Y. and Y.L. acknowledge financial support from the China Scholarship Council (CSC). N.Y.D. acknowledges financial support from the Zernike Bonus Incentive Scheme.

■ REFERENCES

(1) Cheng, Y. J.; Yang, S. H.; Hsu, C. S. Synthesis of Conjugated Polymers for Organic Solar Cell Applications. *Chem. Rev.* **2009**, *109*, 5868−5923.

(2) Heeger, A. J. Semiconducting Polymers: The Third Generation. *Chem. Soc. Rev.* **2010**, *39*, 2354−2371.

(3) Heeger, A. J. 25th Anniversary Article: Bulk Heterojunction Solar Cells: Understanding the Mechanism of Operation. *Adv. Mater.* **2014**, *26*, 10−28.

(4) Guo, X.; Facchetti, A.; Marks, T. J. Imide- And Amide-Functionalized Polymer Semiconductors. *Chem. Rev.* **2014**, *114*, 8943−9012.

(5) Dou, L.; Liu, Y.; Hong, Z.; Li, G.; Yang, Y. Low-Bandgap Near-Ir Conjugated Polymers/Molecules for Organic Electronics. *Chem. Rev.* **2015**, *115*, 12633−12665.

(6) Liu, C.; Wang, K.; Gong, X.; Heeger, A. J. Low Bandgap Semiconducting Polymers for Polymeric Photovoltaics. *Chem. Soc. Rev.* **2016**, *45*, 4825−4846.

(7) Meng, L.; Zhang, Y.; Wan, X.; Li, C.; Zhang, X.; Wang, Y.; Ke, X.; Xiao, Z.; Ding, L.; Xia, R.; Yip, H.-L.; Cao, Y.; Chen, Y. Organic and Solution-Processed Tandem Solar Cells With 17.3% Efficiency. *Science* **2018**, *361*, 1094−1098.

(8) Duan, C.; Zhang, K.; Zhong, C.; Huang, F.; Cao, Y. Recent Advances in Water/Alcohol-Soluble P-Conjugated Materials: New Materials and Growing Applications in Solar Cells. *Chem. Soc. Rev.* **2013**, *42*, 9071−9104.

(9) Chueh, C. C.; Li, C. Z.; Jen, A. K. Recent Progress and Perspective in Solution-Processed Interfacial Materials for Efficient and Stable Polymer and Organometal Perovskite Solar Cells. *Energy Environ. Sci.* **2015**, *8*, 1160−1189.

(10) Xu, B.; Hou, J. Solution-Processable Conjugated Polymers as Anode Interfacial Layer Materials for Organic Solar Cells. *Adv. Energy Mater.* **2018**, *8*, 1800022.

(11) Ye, L.; Xiong, Y.; Zhang, Q.; Li, S.; Wang, C.; Jiang, Z.; Hou, J.; You, W.; Ade, H. Surpassing 10% Efficiency Benchmark for Nonfullerene Organic Solar Cells by Scalable Coating in Air From Single Nonhalogenated Solvent. *Adv. Mater.* **2018**, *30*, 1705485.

(12) Jiang, H.; Taranekar, P.; Reynolds, J. R.; Schanze, K. S. Conjugated Polyelectrolytes: Synthesis, Photophysics, and Applications. *Angew. Chem., Int. Ed.* **2009**, *48*, 4300−4316.

(13) Duarte, A.; Pu, K. Y.; Liu, B.; Bazan, G. C. Recent Advances in Conjugated Polyelectrolytes for Emerging Optoelectronic Applications. *Chem. Mater.* **2011**, *23*, 501−515.

(14) Zhu, C. L.; Liu, L. B.; Yang, Q.; Lv, F. T.; Wang, S. Water-Soluble Conjugated Polymers for Imaging, Diagnosis, and Therapy. *Chem. Rev.* **2012**, *112*, 4687−4735.

(15) Patil, A. O.; Ikenoue, Y.; Wudl, F.; Heeger, A. J. Water Soluble Conducting Polymers. *J. Am. Chem. Soc.* **1987**, *109*, 1858−1859.

(16) Costa, T.; de Azevedo, D.; Stewart, B.; Knaapila, M.; Valente, A. J. M.; Kraft, M.; Scherf, U.; Burrows, H. D. Interactions of a Zwitterionic Thiophene-Based Conjugated Polymer With Surfactants. *Polym. Chem.* **2015**, *6*, 8036−8046.

(17) Houston, J. E.; Kraft, M.; Mooney, I.; Terry, A. E.; Scherf, U.; Evans, R. C. Charge-Mediated Localization of Conjugated Polythiophenes in Zwitterionic Model Cell Membranes. *Langmuir* **2016**, *32*, 8141−8153.

(18) Liu, Y.; Page, Z. A.; Russell, T. P.; Emrick, T. Finely Tuned Polymer Interlayers Enhance Solar Cell Efficiency. *Angew. Chem., Int. Ed.* **2015**, *54*, 11485−11489.

(19) He, Z.; Xiao, B.; Liu, F.; Wu, H.; Yang, Y.; Xiao, S.; Wang, C.; Russell, T. P.; Cao, Y. Single-Junction Polymer Solar Cells With High Ef Fi Ciency and Photovoltage. *Nat. Photonics* **2015**, *9*, 174−179.

(20) Seo, J. H.; Gutacker, A.; Walker, B.; Cho, S.; Garcia, A.; Yang, R.; Nguyen, T.-q.; Heeger, A. J.; Bazan, G. C. Improved Injection in N-Type Organic Transistors With Conjugated Polyelectrolytes. *J. Am. Chem. Soc.* **2009**, *131*, 18220−18221.

(21) Seo, J. H.; Gutacker, A.; Sun, Y.; Wu, H.; Huang, F.; Cao, Y.; Scherf, U.; Heeger, A. J.; Bazan, G. C. Improved High-Efficiency Organic Solar Cells via Incorporation of a Conjugated Polyelectrolyte Interlayer. *J. Am. Chem. Soc.* **2011**, *133*, 8416−8419.

(22) Lee, B. H.; Lee, J.-h.; Jeong, S. Y.; Park, S. B.; Lee, S. H.; Lee, K. Broad Work-Function Tunability of P-Type Conjugated Polyelectrolytes for Effi Cient Organic Solar Cells. *Adv. Eng. Mater.* **2015**, *5*, 1401653.

(23) Lee, J.-h.; Lee, B. H.; Jeong, S. Y.; Park, S. B.; Kim, G.; Lee, S. H.; Lee, K. Radical Cation − Anion Coupling-Induced Work Function Tunability in Anionic Conjugated Polyelectrolytes. *Adv. Eng. Mater.* **2015**, *5*, 1501292.

(24) He, Z.; Zhong, C.; Huang, X.; Wong, W. Y.; Wu, H.; Chen, L.; Su, S.; Cao, Y. Simultaneous Enhancement of Open-Circuit Voltage, Short-Circuit Current Density, and Fill Factor in Polymer Solar Cells. *Adv. Mater.* **2011**, *23*, 4636−4643.

(25) Duan, C.; Zhang, K.; Guan, X.; Zhong, C.; Xie, H.; Huang, F.; Chen, J.; Peng, J.; Cao, Y. Conjugated Zwitterionic Polyelectrolyte-Based Interface Modification Materials for High Performance Polymer Optoelectronic Devices. *Chem. Sci.* **2013**, *4*, 1298−1307.

(26) He, Z.; Wu, H.; Cao, Y. Recent Advances in Polymer Solar Cells: Realization of High Device Performance by Incorporating Water/Alcohol-Soluble Conjugated Polymers as Electrode Buffer Layer. *Adv. Mater.* **2014**, *26*, 1006−1024.

(27) Brendel, J. C.; Schmidt, M. M.; Hagen, G.; Moos, R.; Thelakkat, M. Controlled Synthesis of Water-Soluble Conjugated Polyelectrolytes Leading to Excellent Hole Transport Mobility. *Chem. Mater.* **2014**, *26*, 1992−1998.

(28) Henson, Z. B.; Zhang, Y.; Nguyen, T.-q.; Seo, J. H.; Bazan, G. C. Synthesis and Properties of Two Cationic Narrow Band Gap Conjugated Polyelectrolytes. *J. Am. Chem. Soc.* **2013**, *135*, 4163−4166.

(29) Wang, S.; Bazan, G. C. Solvent-dependent aggregation of a water-soluble poly (fluorene) controls energy transfer to chromophore-labeled DNA. *Chem. Commun.* **2004**, 2508−2509.

DOI: 10.1021/acsaem.8b02226
ACS Appl. Energy Mater. 2019, 2, 2197−2204

(30) Mai, C.-k.; Arai, T.; Liu, X.; Fronk, S. L.; Su, G. M.; Segalman, R. A.; Chabinyc, L.; Bazan, G. C. Electrical properties of doped conjugated polyelectrolytes with modulated density of the ionic functionalities. *Chem. Commun.* **2015**, *51*, 17607−17610.
(31) Zhou, H.; Zhang, Y.; Mai, C.-K.; Collins, S. D.; Nguyen, T.-Q.; Bazan, G. C.; Heeger, A. J. Conductive Conjugated Polyelectrolyte as Hole-Transporting Layer for Organic Bulk Heterojunction Solar Cells. *Adv. Mater.* **2014**, *26*, 780−785.
(32) Zhou, H.; Zhang, Y.; Mai, C.-k.; Seifter, J.; Nguyen, T.-q.; Bazan, G. C.; Heeger, A. J. Conjugated Polyelectrolyte Improves Interfacial Contact in Organic Solar Cells. *ACS Nano* **2015**, *9*, 371−377.
(33) Wu, Z.; Sun, C.; Dong, S.; Jiang, X.-f.; Wu, S.; Wu, H.; Yip, H.-l.; Huang, F.; Cao, Y. N-Type Water/Alcohol-Soluble Naphthalene Diimide-Based Conjugated Polymers for High-Performance Polymer Solar Cells. *J. Am. Chem. Soc.* **2016**, *138*, 2004−2013.
(34) Sun, C.; Wu, Z.; Hu, Z.; Xiao, J.; Zhao, W.; Li, H. W.; Li, Q. Y.; Tsang, S. W.; Xu, Y. X.; Zhang, K.; Yip, H. L.; Hou, J.; Huang, F.; Cao, Y. Interface Design for High-Efficiency Non-Fullerene Polymer Solar Cells. *Energy Environ. Sci.* **2017**, *10*, 1784−1791.
(35) Jia, J.; Fan, B.; Xiao, M.; Jia, T.; Jin, Y.; Li, Y.; Huang, F.; Cao, Y. N-Type Self-Doped Water/Alcohol-Soluble Conjugated Polymers With Tailored Energy Levels for High-Performance Polymer Solar Cells. *Macromolecules* **2018**, *51*, 2195−2202.
(36) Duan, C.; Cai, W.; Hsu, B. B. Y.; Zhong, C.; Zhang, K.; Liu, C.; Hu, Z.; Huang, F.; Bazan, G. C.; Heeger, A. J.; Cao, Y. Toward Green Solvent Processable Photovoltaic Materials for Polymer Solar Cells: The Role of Highly Polar Pendant Groups in Charge Carrier Transport and Photovoltaic Behavior. *Energy Environ. Sci.* **2013**, *6*, 3022−3034.
(37) Chiechi, R. C.; Sonmez, G.; Wudl, F. A Robust Electroactive N-Dopable Aromatic Polyketone. *Adv. Funct. Mater.* **2005**, *15*, 427−432.
(38) Voortman, T. P.; De Gier, H. D.; Havenith, R. W.; Chiechi, R. C. Stabilizing Cations in the Backbones of Conjugated Polymers. *J. Mater. Chem. C* **2014**, *2*, 3407−3415.
(39) Voortman, T. P.; Bartesaghi, D.; Koster, L. J. A.; Chiechi, R. C. Cross-Conjugated N-Dopable Aromatic Polyketone. *Macromolecules* **2015**, *48*, 7007−7014.
(40) Voortman, T. P.; Chiechi, R. C. Thin Films Formed From Conjugated Polymers With Ionic, Water-Soluble Backbones. *ACS Appl. Mater. Interfaces* **2015**, *7*, 28006−28012.
(41) Bartholome, D.; Klemm, E. Novel Polyarylene-Triarylmethane Dye Copolymers. *Macromolecules* **2006**, *39*, 5646−5651.
(42) Dumsch, I.; Kudla, C. J.; Scherf, U. Polytriarylamines With On-Chain Crystal Violet Moieties. *Macromol. Rapid Commun.* **2009**, *30*, 840−844.
(43) Frisch, M. J.; Trucks, G. W.; Schlegel, H. B.; Scuseria, G. E.; Robb, M. A.; Cheeseman, J. R.; Scalmani, G.; Barone, V.; Petersson, G. A.; Nakatsuji, H.; Li, X.; Caricato, M.; Marenich, A. V.; Bloino, J.; Janesko, B. G.; Gomperts, R.; Mennucci, B.; Hratchian, H. P.; Ortiz, J. V.; Izmaylov, A. F.; Sonnenberg, J. L.; Williams-Young, D.; Ding, F.; Lipparini, F.; Egidi, F.; Goings, J.; Peng, B.; Petrone, A.; Henderson, T.; Ranasinghe, D.; Zakrzewski, V. G.; Gao, J.; Rega, N.; Zheng, G.; Liang, W.; Hada, M.; Ehara, M.; Toyota, K.; Fukuda, R.; Hasegawa, J.; Ishida, M.; Nakajima, T.; Honda, Y.; Kitao, O.; Nakai, H.; Vreven, T.; Throssell, K.; Montgomery, J. A., Jr.; Peralta, J. E.; Ogliaro, F.; Bearpark, M. J.; Heyd, J. J.; Brothers, E. N.; Kudin, K. N.; Staroverov, V. N.; Keith, T. A.; Kobayashi, R.; Normand, J.; Raghavachari, K.; Rendell, A. P.; Burant, J. C.; Iyengar, S. S.; Tomasi, J.; Cossi, M.; Millam, J. M.; Klene, M.; Adamo, C.; Cammi, R.; Ochterski, J. W.; Martin, R. L.; Morokuma, K.; Farkas, O.; Foresman, J. B.; Fox, D. J. *Gaussian 09*, revision B.01; Gaussian Inc.: Wallingford, CT, 2009.
(44) Patel, S. N.; Javier, A. E.; Stone, G. M.; Mullin, S. A.; Balsara, N. P. Simultaneous Conduction of Electronic Charge and Lithium Ions in Block Copolymers. *ACS Nano* **2012**, *6*, 1589−1600.
(45) Sariciftci, N. S.; Braun, D.; Zhang, C.; Srdanov, V. I.; Heeger, A. J.; Stucky, G.; Wudl, F. Semiconducting Polymer-Buckminsterfullerene Heterojunctions: Diodes, Photodiodes, and Photovoltaic Cells. *Appl. Phys. Lett.* **1993**, *62*, 585−587.
(46) Yu, G.; Gao, J.; Hummelen, J. C.; Wudl, F.; Heeger, A. J. Polymer Photovoltaic Cells - Enhanced Efficiencies via a Network of Internal Donor-Acceptor Heterojunctions. *Science* **1995**, *270*, 1789−1791.
(47) Doumon, N. Y.; Wang, G.; Chiechi, R. C.; Koster, L. J. A. Relating Polymer Chemical Structure to the Stability of Polymer:-fullerene Solar Cells. *J. Mater. Chem. C* **2017**, *5*, 6611−6619.

DOI: 10.1021/acsaem.8b02226
ACS Appl. Energy Mater. 2019, 2, 2197−2204